Research Article

Marianne Koivulehto, Natalia Battchikova, Saara Korpela, Elvira Khalikova, Anton Zavialov, Timo Korpela*

Comparison of kinetic and enzymatic properties of intracellular phosphoserine aminotransferases from alkaliphilic and neutralophilic bacteria

https://doi.org/10.1515/chem-2020-0014
received January 1, 2020; accepted February 6, 2020.

Abstract: Intracellular pyridoxal 5´-phosphate (PLP) -dependent recombinant phosphoserine aminotransferases (PSATs; EC 2.6.1.52) from two alkaliphilic *Bacillus* strains were overproduced in *Escherichia coli*, purified to homogeneity and their enzymological characteristics were compared to PSAT from neutralophilic *E. coli*. Some of the enzymatic characteristics of the PSATs from the alkaliphiles were unique, showing high and sharp pH optimal of the activity related to putative internal pH inside the microbes. The specific activities of all of the studied enzymes were similar (42-44 U/mg) as measured at the pH optima of the enzymes. The spectrophotometric acid-base titration of the PLP chromophore of the enzymes from the alkaliphiles showed that the pH optimum of the activity appeared at the pH wherein the active sites were half-protonated. Detachment of PLP from holoenzymes did not take place even at pH up to 11. The kinetics of the activity loss at acid and alkaline pHs were similar in all three enzymes and followed similar kinetics. The available 3-D structural data is discussed as well as the role of protons at the active site of aminotransferases.

Keywords: pyridoxal 5´-phosphate dependent enzymes; phosphoserine aminotransferase; protons at the active site of transaminases.

***Corresponding author: Timo Korpela,** Department of Future Technologies, University of Turku, FI 20014, Finland, E-mail: timokor@utu.fi
Marianne Koivulehto, Natalia Battchikova, Saara Korpela, Elvira Khalikova, Anton Zavialov, International Joint Biotechnology Laboratory, MediCity, Faculty of Medicine, University of Turku, Tykistökatu 6A, Turku, FIN-20520, Finland

Abbreviations

PSAT, phosphoserine aminotransferase (EC 2.6.1.52); PLP pyridoxal 5´- phosphate; *PSAT*-BALC, PSAT isolated from *B.alcalophilus*; PSAT-BCIRA, PSAT from *B.circulans* var. *alcalophilus;* PSAT-ECOLI, PSAT from *E.coli*; GlDH, glutamate dehydrogenase (EC1.4.1.3); AspAT, aspartate aminotransferase (2.6.1.1); HPAT, histidinolphosphate aminotransferase; Glu, L-glutamate; 3PHP, phosphohydroxypuryvate; 2-oxo, 2-oxoglutarate; PSer, L-phosphoserine.

1 Introduction

Our laboratory has worked with *Bacillus circulans* var *alcalophilus* since about 1983. It is an alkaliphilic microbe growing optimally at pH values 9.5-10.5. We have isolated and studied several enzymes from that microbe. We found that two aspartate aminotransferases (AspAT) activity peak in an ion exchange chromatographic purification of the microbial supernatant. The major activity peak appeared not to be AspAT but phosphoserine aminotransferase (PSAT) with surprisingly high AspAT side activity [1]. We later isolated AspAT from the minor peak. This AspAT had an exceptional 20-amino acid extension at its functionally important N-terminus [2]. This enzyme was otherwise a typical homo-dimeric enzyme with two active sites. Molecular modelling studies implied that the extension was formed of two pieces of alpha helices lying on active sites partly on both dimer subunits. This prompted us to speculate that AspAT from the alkaliphile has a unique structure enabling it to function in alkaline pH. In spite of large efforts to crystallize AspAT, we failed, and it was deduced that the possible flexible N-terminal extension was the reason. A truncated AspAT was not, however active and existed only at the monomeric stage [3]. Thus, the extension was at least important in maintaining the quaternary structure of the enzyme. Because of the

success with cloning and purification of PSAT we decided to study the ideas raised by AspAT with PSATs.

Crystallization and preliminary X-ray analysis of PSAT, (EC 2.6.1.52) from *B. circulans* was made by Moser et al. [4] in Basel, Switzerland, quite long time before the first PSAT structure from *Escherichia coli* was solved [5]. Further studies on crystal structures of PSAT from *B. circulans* were re-started by Dubnovitsky *et al*. in Turku, Finland, in collaboration with our laboratory [6, 7, 8]. The present study describes in detail the basic protein chemistry and enzyme kinetic properties of PSATs of *B. circulans* and obligate alkaliphile *B. alcalophilus* comparing them with PSAT from *E.coli*. The present study also describes data which are not described in the cited previous papers focused on 3-D structures.

PSAT catalyses the second step of phosphorylated pathway of serine biosynthesis: L-glutamate (Glu) + 3-phosphohydroxypyruvate (3PHP) ⇔ 2-oxoglutarate (2-oxo) + L-phosphoserine (PSer). The catalytic mechanisms and 3-D structures of aminotransferases (AspAT as the spearhead) are described in textbooks. The early studies on transaminases have been reviewed by the scientists who originally discovered the enzyme mechanisms, for example, in the monograph by Christen and Metzler [9], and textbook by Metzler [10]. A special advantage of aminotransferases in studies of alkaline adaptation is the fact that PSATs contain pyridoxal 5´-phosphate (PLP) as the coenzyme which is itself a pH indicator.

Possible adaptation mechanisms of PSAT to alkaline conditions are discussed against the background of the acid-base chemistry of PLP and PLP enzymes with a brief reference to the available 3-D crystal data of PSATs.

2 Materials and methods

2.1 Plasmids

The cloning of the *psat* gene from *B. circulans* was described earlier [1]. To overproduce the protein in *E. coli*, pPSAT-BCIRA plasmid was constructed as follows. In order to change the TTG start codon to ATG and to insert the *Bam*HI site into the 5'-untranslated region of the gene, two-step PCR [11] was performed using oligonucleotides A (5'-GCTCATAAAACTCTCCACCCTTCTCTC-3'), B (5'-CACCGGATCCCACAGCTAACCCTTACCTG-3'), C (5'-CCCAGTCACGACGTTGTAAAACGACG-3') and the plasmid coding the N-terminal part of the protein. pPSAT-BCIRA expression plasmid was obtained by triple ligation of pUC18/*Bam*HI-*Hind*III vector, *Bam*HI-*Eco*RI fragment excised from the PCR product, and *Eco*RI-*Hind*III fragment coding the C-terminal part of the protein. Further, using the *psat* gene from *B. circulans* as a hybridization probe, the *psat* gene from *B. alcalophilus* was cloned (the sequence was submitted to Genbank with the accession number AF204962). To overproduce PSAT from *B. alcalophilus* in *E. coli*, pPSAT-BALC plasmid was constructed as follows. The *Nde*I site was introduced into the start of *psat* coding frame by PCR using oligonucleotides D (5'-TCCCGGATCCATATGGTAAAACAAGTTTTTAACTT-3') and E (5'-AACATAGTAAATTGTAAGCTCGCCC-3'). Finally, *Nde*I-*Sac*I fragment obtained from the PCR product and the *Sac*I-*Cla*I fragment, coding the rest of *B. alcalophilus psat* gene, were cloned into pT7-7 plasmid [12]. DNA manipulations and transformation of *E. coli* were performed according to Sambrook *et.al*., [13].

2.2 Bacterial strains

E. coli strains XL1-blue (Stratagene, La Jolla, USA) and BL21(DE3) (Novagene, Madison, USA) were used as hosts for pPSAT-BCIRA and pPSAT-BALC, respectively. *E. coli* strain AB2829 harbouring pKD501 plasmid [14] was used for isolation of PSAT-ECOLI. This strain was kindly donated to us by Prof. J. Jansonius (University of Basel, Switzerland). Recombinant strains were grown in a Luria-Bertani medium [13] containing ampicillin (50 g/ml).

2.3 Measurement of protein quantities

Protein was measured usually with the method of Bradford [15], using bovine serum albumin as the standard with reagents from Biorad. For pure proteins, absorption at 280 nm was correlated with the amount of protein. A suitable amount of pure protein (2-3 mg) was divided into two equal parts. One was dialyzed against distilled water, lyophilized and dried to constant weight. Absorbance at 280 nm of the soluble part was correlated to the weighted mass of protein. The molar absorptivities of the pure PSATs at 280 nm were about 31000/M x cm ± 1000 (see the Results). They were in harmony of their structural similarities and contents of aromatic amino acid residues. If the purest fractions of the proteins were compared by SDS or IEF gel scans (see e.g. Fig 1, colours of lanes 3-5) their amounts were also the same within accuracy of 5-10%.

2.4 Isolation of recombinant enzymes

PSAT-BALC was isolated from *E. coli* BL21(DE3) recombinant strain harbouring pPSAT-BALC plasmid. Cells were grown in 4 litres of Luria-Bertani medium [13] with ampicillin (70 mg/l) at 18°C and after 3-4 h growth in IPTG (0.1 mM) cells were collected and washed with 0.15 M NaCl. Wet cell pellet was suspended in 25 mM Tris-Cl, pH 7.5-8, 100 μM PLP, 1 mM DTT, 1 mM PMSF and 5 mM EDTA followed by sonication and centrifugation at 20,000 g, at 4°C, for 20 min. Streptomycin sulphate was added to supernatant to get concentration of 1% (w/v) on an ice bath followed by centrifugation at 20,000 g for 20 min. The supernatant was applied onto a DEAE-Sepharose CL-6B (Pharmacia, Sweden) column (2.5 x 30 cm) equilibrated with 25 mM Tris-Cl, pH 7.5-8.0. The chromatography was carried out at 10°C with a linear gradient of NaCl from 0.1 to 0.4 M containing 25 mM Tris-Cl, pH 7.5-8.0, 50 mM PLP and 50 mM NaCl. Fractions from the PSAT-active peak were pooled and concentrated with an Amicon YM-10 Centriprep (Millipore, USA). The enzyme was applied in portions onto a Mono Q HR 5/5 (Pharmacia Biotech, Sweden) FPLC column (1 ml) as a second column equilibrated with 50 mM Tris-Cl, pH 7.5. The chromatography was carried out with a linear gradient of NaCl from 0 to 0.3 M within 30 column volumes at the room temperature. Active fractions were pooled and sterilised by filtration through Tyffryn membrane (0.2 μM) filter (Gelman Sciences, USA). The enzyme was stored on ice-water.

PSAT-BCIRA, Lys (2) Glu mutant, was isolated from *E. coli* XL1-blue recombinant strain harbouring pPSAT-1 plasmid. Cells were grown for 2 hours after IPTG induction (0.5 mM) at 37°C in 2.5 litres of Luria-Bertani medium [13] with ampicillin (50 mg/l). Subsequent steps up to the second chromatography step were as with PSAT-BALC and thereafter PSAT-BCIRA was applied in portions onto a Synchropak AX300 (MICRA Scientific Inc., USA) HPLC column (25 x 0.46 cm) equilibrated with 50 mM Tris-Cl, pH 7.5, 20 μM PLP, 0.01% β-mercaptoethanol, 50 mM NaCl. The chromatography was carried out with a linear gradient of NaCl from 0.3 to 0.9 M within 5 column volumes. After concentration with a PM-10 membrane, the enzyme solution was applied onto a Sephacryl 200HR gel filtration column (1.6 x 80 cm) and eluted with 25 mM Tris-Cl, pH 7.5, 0.1 M NaCl. Active fractions of PSAT-BCIRA were pooled and sterilised by filtration and stored in ice-water.

The isolation of PSAT-ECOLI was performed according to Lewendon [14], except 100 mM PLP was used during cell disruption. PSAT-ECOLI was sterilised by filtration and stored in ice-water.

The molecular mass of the denatured protein was determined for PSAT-BALC and PSAT-BCIRA by SDS-PAGE (12.5%) according to Laemmli [16]. A kit for molecular weights 12,300-78,000 (LKB-Pharmacia, Sweden) was used in SDS-PAGE. The molecular mass of native PSAT-BCIRA was estimated by FPLC size exclusion chromatography on a Superose 6, PC 3.2/30 column (Pharmacia, Sweden). The following molecular mass markers were used: bovine serum albumin (66 kDa), α-amylase (55 kDa), trypsin (23.3 kDa), lysozyme (14.3 kDa).

For the p*I* measurements, Ready PhastGel IEF 4-6.5 (Pharmacia) was used in the PhastSystem (Pharmacia). The following markers were applied: β-lactoglobulin, pI 5.1 (Sigma), trypsin inhibitor, p*I* 4.6 (Sigma), and the isoelectric focusing calibration kit (Pharmacia, Sweden).

The pH dependence on the PSAT-BALC and PSAT-BCIRA activity in the forward reaction (Glu + 3PHP) was measured with a fixed-time assay at 25°C. The PSAT reaction was performed in several buffers (Bis-Tris-propane, CAPS and CHES). The reaction mixture contained 100 mM buffer, 250 mM NaCl, 20 μM PLP, 0.2 μg PSAT, and saturating concentrations of substrates (8 mM Glu, 0.5 mM 3PHP) in a total volume of 0.2 ml. The reaction was initiated with 3PHP and stopped after 3 min by addition 350 ml of 1 M MES, pH 6.1. 2-oxoglutarate produced by PSAT was measured with NADH-dependent glutamate dehydrogenase (GlDH) from bovine liver (Boehringer Mannheim) by adding 0.18 mM NADH, 32 mM ammonium acetate, 12 U GlDH, and water to get the final volume of 1 ml [17]. GlDH is 50% active at pH 6.1. The highest slope value obtained was referred as 100%. To determine the pH dependence of V (in percentage scale) the data were fitted to equation 1.

For the pH-stability/ first-order rate constants for enzyme inactivation vs. pH, PSAT-BALC, PSAT-BCIRA, and PSAT-ECOLI were incubated in 50 mM buffers (citrate, MES, HEPES, borate and carbonate), 250 mM NaCl, and 20 μM PLP at enzyme concentrations of 30 μg/ml. Aliquots of 0.2 mg of enzyme were taken at certain time intervals. The residual enzyme activity was immediately measured by coupling the enzyme reaction with GlDH at 25°C, pH 8.2. The assay mixture (1 ml) contained 200 mM Tris-Cl, pH 8.2, 32 mM ammonium acetate, 8 mM Glu, 20 μM PLP, 0.5 mM 3PHP, 0.18 mM NADH, 12 U GlDH, and 0.5 μg PSAT. The reaction was started with 3PHP and the decrease of absorbance was monitored at 340 nm. The highest slope value obtained was referred as 100%. The pH 8.2 is optimal for GlDH and alkalophilic PSATs has 80 % activity left at this pH.

Table 1: Purification of recombinant phosphoserine aminotransferase of *Bacillus alcalophilus* produced in *E. coli* host cells.

Procedure	Total protein (mg)	Total activity (U)	Specific activity (U/mg)	Purification factor	Yield (%)
Crude extract	88	238	2.7	1	100
DEAE Sepharose	19.4	230	11.9	4.4	97
Mono Q HR 5/5	5.6	73	42	15.6	31

Table 2: Purification of recombinant phosphoserine aminotransferase of *Bacillus circulans* var. *alcalophilus* produced in *E. coli* host cells.

Procedure	Total protein (mg)	Total activity (U)	Specific activity (U/mg)	Purification factor	Yield (%)
Crude extract	1002	8116	8.1	1	100
DEAE Sepharose	189	5273	27.9	3.4	65
Synchropak AX300	83.5	2839	34.0	4.2	35
Sephacryl 200 HR	72	2477	44.4	5.5	31

The pH dependence of the absorption spectra of PSAT-BALC and PSAT-BCIRA were measured with a BioSpec-1601 E spectrophotometer (Shimadzu, Japan), in a 1 cm quartz cuvette at protein concentrations of 25 mM and 10 mM for PSAT-BALC and PSAT-BCIRA, respectively, in a buffer solution (50 mM Bis-Tris-propane pH 6.3 - 9.5 or CAPS pH 10 – 11.5) containing 250 mM NaCl.

To determine the kinetic parameters of the Glu/3PHP pair, matrices of initial rate data at four to five concentrations of each substrate were collected. PSAT-BCIRA activities were measured like in the item 'the pH dependence of the PSAT-BALC and PSAT-BCIRA activity', except PSAT reaction was performed at pH 8.2 in Bis-Tris-propane, at pH 9.5 in CHES and without NaCl.

Amino acid analysis and protein homology modelling were performed by DeepView/Swiss-PdbViewer (version 3.7) and Swiss-Model (version 36.0003) [18, 19, 20].

Ethical approval: The conducted research is not related to either human or animal use.

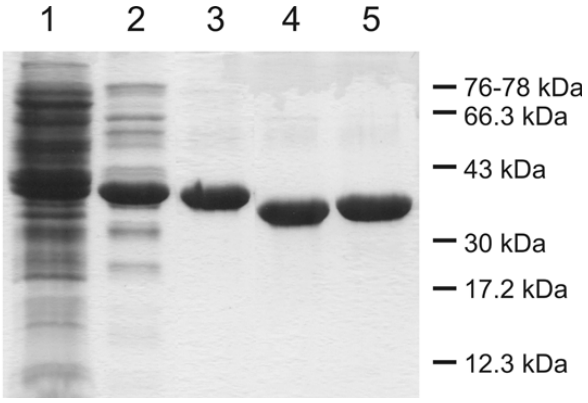

Figure 1: 12.5% SDS-PAGE. PSAT-BALC on lane 1 (crude extract; 20 µg/lane), 2 (the same after DEAE Sepharose CL-6B; 8 µg/lane), and 3 (the same after Mono Q HR 5/5; 5 µg/lane); Final purified PSAT-BCIRA lane 4 (5µg/lane), and PSAT-ECOLI lane 5 (5µg/lane). See also Tables 1 and 2. Position of the molecular weight markers 12.3-78 kDa (LKB-Pharmacia) are shown on the right.

3 Results

3.1 Purification and characterisation of the recombinant proteins

The *psat* genes of *B. alcalophilus* and *B. circulans* were cloned in *E. coli* expression vectors resulting in pPSAT-BALC and pPSAT-BCIRA, respectively. The pPSAT-BALC plasmid coded for the authentic *B. alcalophilus* enzyme, while pPSAT-BCIRA encoded the Lys (2) Glu mutant of the *B. circulans* enzyme (other transformants were unstable). The enzymes were purified to near-homogeneity (Figure 1, Lanes 2-4, Tables 1-2). The purities of PSAT-BALC, PSAT-BCIRA and PSAT-ECOLI recombinant enzymes were about the same (Figure 1), and hence all the used preparations were comparable.

Apparent molecular masses (M_r) of the denatured proteins obtained by SDS-PAGE were 39.5-40.5 and 38-39.8 kDa for PSAT-BALC and PSAT-BCIRA, respectively (Figure 1), that agreed well with theoretical calculations 40,200 Da for PSAT-BALC and 39,793 Da for PSAT-BCIRA. M_r of

Table 3: Comparison of properties of phosphoserine aminotransferases from various sources. The data marked with asterisks were determined with the near-homogenous recombinant enzymes of the present study. Upper numeral indexes refer to the source of the data: [1] [37]; [2] [53]; [3] [54]; [4] [55]; [5] [56]; [6] [57]; [7] [58]; [8] [59]; [9] [9]; [10] [10]; [11] [17].

Enzyme PSAT	MW (kDa)	pH optimum	p*I*	K_m (μM)	specific activity (U/mg)	p*K* (internal aldimine)	UV maxima (nm)	ε_M ($M^{-1}cm^{-1}$)
B. alkalophilus	[*]39.5-40.5 (SDS-PAGE); 40,200 (360 aa)	[*]Sharp optimum at 9.4	[*]4.6	n.d.	[*]42 (pH 9.5, 25°C)	[*]9.44	[*]410 (pH<9.4) and 345 (pH>9.4)	[*]29540 (280 nm); 3855 (345 nm); 4330 (410 nm)
***B. circulans* var. *alkalophilus* Lys(2)Glu**	[*]38-39.5 (SDS-PAGE); [5]39,793 (361 aa); [*]66 (FPLC GF)	[*]Sharp optimum at 9.5	[*]4.6	[*]3PHP: 17.3 (pH 9.5), 1.7 (pH 8.2); Glu: 800 (pH 9.5), 1.4 x 10^3 (pH 8.2)	[*]44.4 (pH 9.5, 25°C)	[*]9.55	[*]412 (pH<9.5) and 348 (pH>9.5)	(*)32100 (280 nm); 21570 (348); 21880 (412 nm)
***E. coli* B**	[1]79.8-81.2	n.d.	n.d.	[1]PSer: 1.4 x 10^3; 2-oxo: 67	[1] 3.8 (reverse) at 25°C with 3-PGDH and DPNH	n.d.	[1]405 and 320 (neutral pH)	n.d.
***E. coli* K12**	[2]39-40 (SDS-PAGE); [3]39,834 (362 aa); [2]68 (HPLC GF)	[4]Broad maximum between 7.5 and 8.5	[*]4.6	[2]3PHP: 4.0; Glu: 1.2 x 10^3	[2] 16.2; [*] 42.3 (pH 8.2, 25°C)	[4]8.40	[4]408 (pH<8.4) and 340 (pH>8.4)	n.d.
Beef liver	[8] 43 (SDS-PAGE); 77 (Sephacryl 200); 90.7 (sedimentation)	[6]6.8-7.2	n.d.	[6] 3PHP: 5; Glu: 1.2 x 10^3	[8]14-16 (38°C)	n.d.	n.d.	n.d.
Sheep brain	[7]96 (sedimentation)	[7] relatively sharp optimum at 8.15	n.d.	[7] 3PHP: 250; L-Glu: 700 (pH 8.2)	[7]1.3 (25°)	n.d.	[7] 415, moves to 330 with $NaBH_4$ at pH 5.5	n.d.
Green alga *Scenedesmus obliquus*, mutant C-2 A'	[9] 40 (SDS-PAGE); 80 (Fractogel HW55)	[10] 6.8-8.2	n.d.	[10]PSer: 83; 2-oxo: 180	[9]13.8 (reverse) at 30°C with P-glycerate DHG and NADH	n.d.	[9] 390-410 (pH 7.6)	n.d.
Soybean root nodules	[11] 85 (Sepharose CL-6B)	[11] plateau between pH 7.5-9	n.d.	[11]Glu: 500; 3PHP: 60	[11] 7	n.d.	n.d.	n.d.

the native PSAT-BCIRA was 66 kDa according to FPLC size exclusion chromatography (data not shown). Thus, PSAT-BCIRA is a homodimer typical for transaminases. The α2-dimeric form of PSAT-BCIRA was further confirmed by X-ray studies (Protein Data Bank accession code 1BT4).

IEF-PAGE showed the same p*I* value of 4.6 for PSAT-BCIRA[Lys(2)Glu], PSAT-BALC and PSAT-ECOLI implying that the average surface charge was equal.

3.2 Specific activity

Three near-homogenous enzymes in similar optimized assay conditions were compared (see Methods). Specific activities of PSAT-BALC and PSAT-BCIRA were 42.0 U/mg and 44.4 U/mg, in that order, when determined at their optimal pHs (25°C). These values are notably higher than those reported for PSATs from other sources (Table 3). E.g.,

for PSAT from sheep brain had a specific activity of 1.3 U/mg as determined at pH 8.2 (25°C) [17]. For PSAT from bovine liver the value of 14-16 U/mg was obtained at pH 7.0 (38°C) [21]. Specific activity of 16.2 U/mg was obtained for even recombinant PSAT-ECOLI at pH 8.2 (25°C) [14], whereas we obtained specific activity of 42.3 U/mg. The difference in these values is likely due to the purification procedure. We found that the overproduced enzyme is not saturated with PLP *in vivo*. Therefore, we included high concentration of PLP at the step of cell disruption. The shortage of PLP causes an inadequate formation of the dimer. PLP could also bind slightly wrongly at the active site like with beta and gamma forms of AspAT [see ref. 9, p. 138 and elsewhere] showing lower activity. Such sub-forms exist naturally but their role is not yet fully understood.

3.3 pH dependence of catalytic activity

For determination of a pH-dependence of PSAT activity, PSAT and GlDH reactions were carried out separately to exclude the influence of pH on the GlDH activity. Measurements were carried out in various buffers.

As seen in Figure 2B, the data for the apparent V_{max} of PSAT-BCIRA fit well into the equation [22]:

$$\log V_{maxapp} = \log V_{max} - \log(1 + [H]/K_{es1} + K_{es2}/[H]) \quad (1)$$

where V_{maxapp} is the apparent V_{max}, and V_{max} is the pH-independent theoretical maximal velocity and [H] stands for the hydrogen ion concentration. K_{es1} and K_{es2} are two successive ionization constants for the enzyme-substrate complex. Bell-shaped curves have slopes of +1 and –1 on the acidic and basic sides, respectively, indicating dependence of two ionizing groups in the enzyme-substrate complex (diprotic model). The pK_{es1} values were obtained by fitting the experimental data in the plot of $1/V_{maxapp}$ vs. [H], and pK_{es2} values from the plot $1/V_{maxapp}$ vs. 1/[H]; the range of [H] were chosen so that the replots were linear [23]. The equation for the replot is:

$$1/V_{maxapp} = 1/(V_{max}K_{es1}) \text{ x } [H] + K_{es2}/(V_{max}) \text{ x } 1/[H] + 1/(V_{max}) \quad (2)$$

The pK_{es} values obtained from $1/V_{maxapp}$-axis intercept replots for PSAT-BCIRA were 8.27 ± 0.05 and 10.67 ± 0.02.

Since pK_{es} values for the PSAT-BALC-substrate complex were separated by less than 2 pH units (Figure 2A), V_{maxapp} and V_{max} cannot be considered identical. A procedure by Alberty and Massey [24]was used to determine pK_{es1} and pK_{es2}, for PSAT-BALC. In this method, the kinetic value plotted was called observed V_{max} (V_{maxobs})

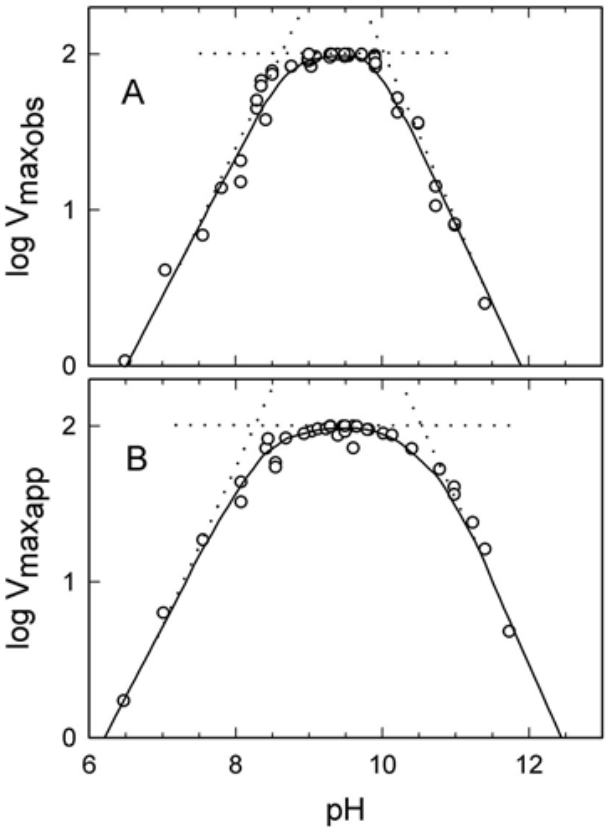

Figure 2: The pH dependence of the catalytic activity for the forward reaction: glutamate + 3-phosphohydroxypyruvate -> 2-oxoglutarate + phosphoserine for PSAT-BALC (A) and of PSAT-BCIRA (B). The experimental data are fitted to theoretical curves as described in the text. The pH optima 9.4 and 9.5 for PSAT-BALC and PSAT-BCIRA were obtained, respectively.

instead of V_{maxapp} to differentiate between the peak value, $V_{maxapp,}$ and the theoretical maximal velocity, indicated as V_{max}. The optimum pH occurs at 1/2(pK_{es1} + pK_{es2}). The observed V_{max} is given by:

$$V_{maxobs} = V_{max}\, K_{es1}\, [H]/(K_{es1}\, [H] + [H]^2 + K_{es1}K_{es2}) \quad (3)$$

The curve, where V_{maxobs} is plotted against pH (data not shown), rises to a maximum at a pH (pH_0) halfway between the two pK_{es} values, 1/2(pK_{es1} + pK_{es2}), which means that

$$[H]_0 = \sqrt{(K_{es1}K_{es2})} \quad (4)$$

in which $[H]_0$ is the H^+ ion concentration at the pH optimum. In the case when $[H] = [H]_{0,}$ one-half V_{maxapp} can be expressed by substitution of equation 4 into equation 3:

$$1/2\, V_{maxapp} = V_{max}/[2 + 4\sqrt{(K_{es2}/K_{es1})}] \quad (5)$$

or

$$1/2\ V_{maxapp} = V_{max}\,[H]_{1/2}K_{es1}/(K_{es1}\,[H]_{1/2} + [H]_{1/2}{}^2 + [H]_0{}^2) \quad (6)$$

Setting equation 5 equal to equation 6 results equation 7:

$$[H]_{1/2}{}^2 - (K_{es1} + 4[H]_0)[H]_{1/2} + [H]_0{}^2 = 0 \quad (7)$$

This equation has two real roots ${}_1[H]_{1/2}$ and ${}_2[H]_{1/2}$, which correspond the [H] at 1/2 V_{maxapp} on each side of the curve. The sum of the two roots can be given as equation 8:

$${}_1[H]_{1/2} + {}_2[H]_{1/2} = K_{es1} + 4[H]_0 \quad (8)$$

While ${}_1[H]_{1/2}$, ${}_2[H]_{1/2}$ and $[H]_0$ can be obtained from the plot of V_{maxobs} vs. pH, the K_{es1} can be calculated from equation 8, K_{es2} from 4 and V_{max} from 5. Calculated pK_{es} values for PSAT-BALC were 8.7±0.16 and 10.3 ±0.16. This shows that these two alkali-active enzymes slightly differ from each other in the protonation mode.

Observed enzyme activity versus pH curve showed a sharp pH optima for PSAT-BALC and PSAT-BCIR at pH 9.4 and 9.5, respectively. As seen from Table 3, the activity of PSAT-BALC and PSAT-BCIRA in alkaline region is exceptional among other PSATs. For example, PSAT-ECOLI has a broad peak of activity at pH 7.5-8.5 [25], PSAT from bovine liver at pH 6.8-7.2 [26], PSAT from green algae at pH 6.8-8.2 [27]. A plateau optimum at pH 7.5-9.0 occurs for activity of PSAT from soybean root nodules [28], while PSAT from sheep brain has a rather sharp optimum of activity at pH 8.15 [17].

Results in Figure 3 show that different buffer anions significantly affected the enzyme activity in the forward reaction. PSAT-BCIRA showed higher activities in CHES, 30% more than CAPS, and almost 40% more than BTP, while PSAT-BALC had slightly higher activities in CAPS than in CHES and BTP (about 10 %). Even the pH optima of the two studied PSATs from alkaliphiles were similar, their kinetics differed from each other. Their molar absorptivities also differed significantly. This reflects the different conjugation of the double bond chain of PLP. This observation is important and will need further studies.

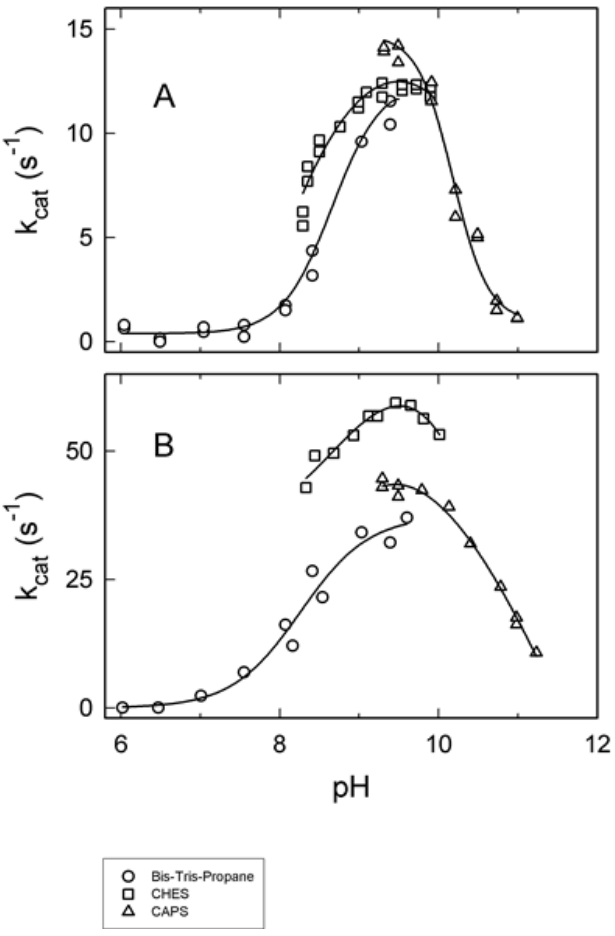

Figure 3: Buffer effect for the glutamate + 3-phosphohydroxypyruvate -> 2-oxoglutarate + phosphoserine reaction of PSAT-BALC (A), and PSAT-BCIRA (B). The PSAT reaction mixture contained 100 mM Bis-Tris-propane (○), CHES (□), and CAPS (Δ); in 250 mM NaCl, 20 µM PLP,and 0.2 µg enzyme. The reaction was stopped after 3 min by changing pH to 6.1 with 1 M MES. 2-Oxoglutarate produced by PSAT was measured with the GlDH reaction. The points are the experimental, while the lines are fitted with the Sigma Plot program (version 6, Jandel Scientific Software).

3.4 pH stability of the protein fold

The slope of the inactivation curve, obtained from log percentage of residual activity against preincubation time at different pHs (data not shown), represents the first-order rate constant k (min^{-1}) for the enzyme inactivation. Data fitted into the plot $t_{1/2}$ ($t_{1/2}$ = 0.6931og k) vs. pH produced linear curves in a log scale (Figure 6). The acidic and alkaline side curves were symmetrical implying to similar rate constants for the irreversible inactivation at both of the pH extremes.

3.5 Effect of pH on electronic spectra of PSATs

PSAT-BALC and PSAT-BCIRA showed pH-dependent electronic absorption spectra (Figure 4A and 4B). At the alkaline side, the absorption maxima of PSAT-BALC and PSAT-BCIRA were at 345 nm and at 348 nm, respectively, whereas at neutral the pH absorption maxima shifted, due to protonation of the aldimine bond, to 410 nm and

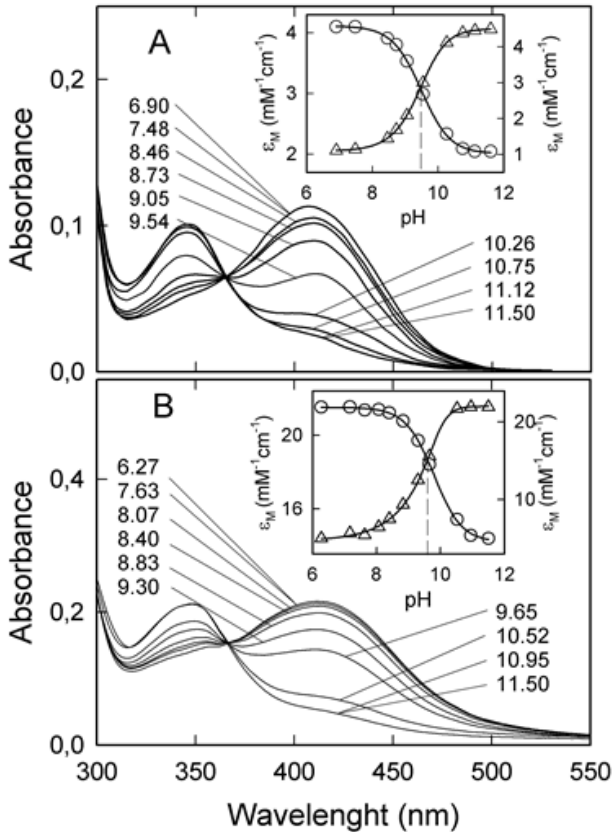

Figure 4: Absorption spectra of the PLP-form enzymes, PSAT-BALC (A) and PSAT-BCIRA (B) at pHs indicated in the figure. Changes in the molar absorptivities at 345 nm (○) and 410 nm (Δ) for PSAT-BALC (A); and 348 nm (○) and 412 nm (Δ) for PSAT-BCIR (B) are plotted against pHs in the insets. Solid lines in the inset are the theoretical curves, obtained by equation 4 (see Results). The internal aldimine showed pK values at 9.4 for PSAT-BALC (A) and 9.5 for PSAT-BCIRA (B). The buffers were 100 mM Bis-Tris-propane (pH 5.9 - 9.6) and CAPS (pH 10.4 - 11.6). Distinct isosbestic points show that only two species are involved.

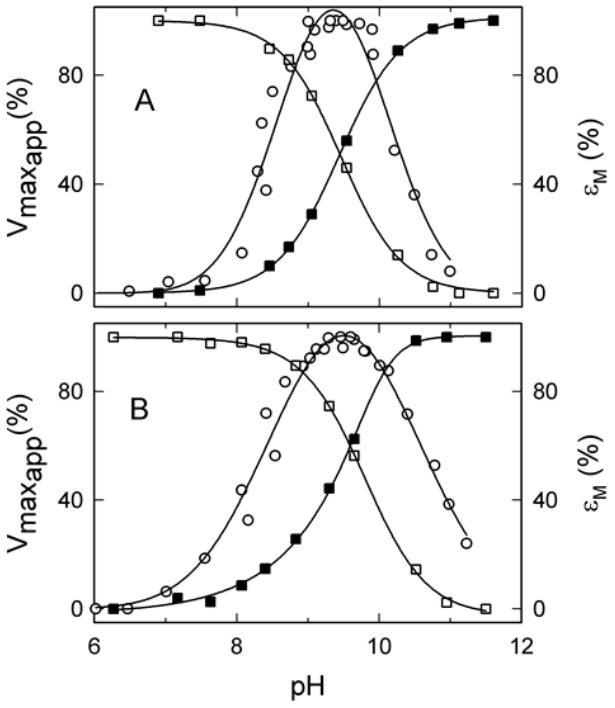

Figure 5: The normalized experimental data of Glu + 3-PHP reaction of activity and spectral data of Figure 4 drawn in the same figure showing that pK of the internal aldimine and optimum activity overlap: PSAT-BALC (A) and PSAT-BCIRA (B).

412 nm, respectively, as with aspartate aminotransferases (AspAT) [29]. The molar absorptivities (ε_M) for PSAT-BALC and PSAT-BCIRA at 280 nm were 29540 and 32100, respectively. The ε_M values were calculated from the Beer-Lambert equation:

$$A = \varepsilon_M \times c \times l \quad (9)$$

in which c is the molar protein concentration (M) and l is the light path in cuvette (1 cm). Since the spectral curves of PSAT-BALC and PSAT-BCIRA at various pHs showed sharp isosbestic points at 365nm and 367 nm respectively (Figure 5A and 5B), the apoenzyme-bound cofactor is in equilibrium in only two of the ionic forms derived from protonation of the internal aldimine nitrogen. The pK_a values of protonation and deprotonation of the coenzyme-lysine aldimine were 9.4 for PSAT-BALC and 9.5 for PSAT-BCIRA (Figure 5A and 5B, inset). The pK_a value of the chromophore was determined by the least squares analysis of the equation:

$$pK_a = pH + \log[(A - A_2)/(A_1 - A)] \quad (10)$$

where A_1 and A_2 are absorbance maxima of acid and basic forms of the enzyme, respectively, and A is observed absorbance at different pHs.

Noteworthy, the pK_a values of the PLP chromophores almost coincided with the catalytic pH optima with both of the enzymes (Figure 5A and 5B). Hence, the imine nitrogen of the internal aldimine is half-protonated at the pH optimum of activity. In comparison, PSAT-ECOLI is about 90 % protonated at its pH-optimum (7.5-8.5) [5] and most of the other aminotransferases remain protonated at their catalytic pH optima [25, 30,31]. AspAT and histidinol phosphate aminotransferase (HPAT) have an exceptionally low pK_a of internal aldimine (6.5-6.8) [32]. It was assumed for theoretical reasons that AspAT gets a proton required for the transimination step from the protonated substrate [33, 34]. With the alkali-active PSATs the optimum pH is presumably acquired by a compromise of pK_a of substrate

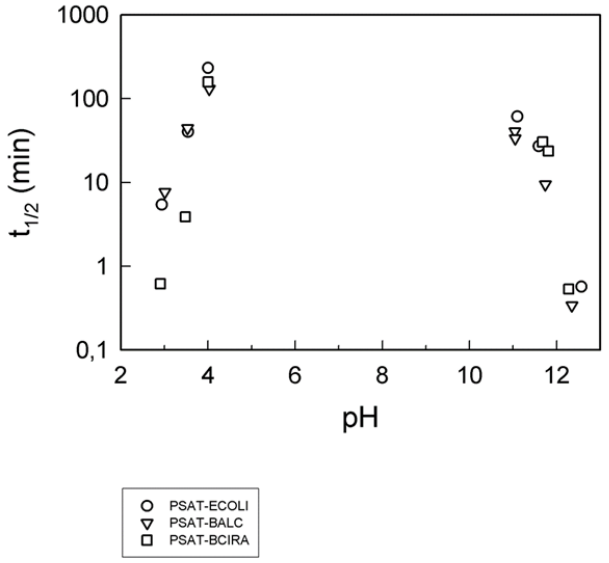

Figure 6: Effect of pH on stability of PSAT-BALC, PSAT-BCIRA and PSAT-ECOLI. 30 µg/ml of PSAT-BALC (Δ), PSAT-BCIRA (□), and PSAT-ECOLI (○) were exposed to 50 mM buffers (citrate, MES, HEPES, borate and carbonate) with 250 mM NaCl (to buffer ionic strength), and 20 µM PLP for 5 – 60 min. At certain time intervals aliquots of enzyme (0.35 µg) were taken and mixed with 200 mM Tris-Cl, pH 8.2, 8 mM Glu, 32 mM ammonium acetate, 250 mM NaCl, and 20 µM PLP. The residual PSAT activity was immediately measured in coupled reaction by adding 10 mM NADH, 24 U GlDH, and 18 mM 3PHP. The slope of inactivation curve, obtained from log percentage of residual activity against preincubation time at different pH values (data not shown), represents the first-order rate constant k (min^{-1}) for enzyme inactivation. In this figure obtained data is fitted into plot of $t_{1/2}$ versus pH in log scale, $t_{1/2} = 0.6931og\ k$. Figure illustrates little differences in $t_{1/2}$ among PSATs (note the log scale). Furthermore, the inactivation curves were symmetrical at the pH extremes (not shown).

amino group and that of the internal aldimine and thus about a half of the required protons are conserved at the active site and half of them come with PSer substrate. The protonation stage of the internal aldimine determines the conformation around the imine nitrogen or vice versa, while the conformation determines its $pK_{a..}$

3.6 Usage of amino acids in PSATs

Amino acid analysis of PSAT-BALC, PSAT-BCIRA, PSAT-ECOLI and PSAT from *B. subtilis* (a neutralophile) revealed a decrease of charged amino acids (Asp, Glu, Arg and Lys), and an increase of neutral hydrophilic amino acids (Asn, Gln and His; pK_a of imidazolium of His is 6, thus in alkaline conditions His is neutral) in alkali-active enzymes (Table 4). The number of neutral amino acids seems to correlate with the microbe's requirement for the elevated pH optimum of catalysis. The usage of amino acids is, however, a poor parameter for forecasting the function since there are a great many combinations of contact networks which could be used to get the same effect. Site-directed mutagenesis studies have shown the complexity of the interpretation of such data. A related problem exists also in interpretation of the 3-D data, i.e. what is specific to achieve a certain function and what is just another way to arrange the same function.

3.7 Kinetic parameters

The kinetic parameters for PSAT-BCIRA were determined for the forward reaction (Glu+3PHP) at pHs 8.2 and 9.5. The data were plotted in 3D diagram, $1/v$ vs. $1/[A]$ vs. $1/[B]$. The K_m and V_{max} were generated from the matrix using equation describing the ping-pong bi-bi mechanism [35]:

$$v/V_{max} = [A][B]/(K_{mB}[A] + K_{mA}[B] + [A][B]) \qquad (11)$$

Parameter v represents initial velocity and V_{max} maximum velocity (M s^{-1}). Symbols [A] and [B] indicate molar (M) concentrations of Glu and 3PHP, respectively. K_{mA} is the Michaelis constant for Glu and K_{mB} for 3PHP. At pH 8.2 K_m values of 1.4 mM and 1.7 µM were calculated for Glu and for 3PHP, respectively. K_m values obtained at pH optimum, 9.5, were 0.8 mM for Glu and 17.3 µM for 3PHP. When compared with PSAT from other sources, substrate affinities of PSAT-BCIRA at pH-optimum are closely related to K_m values reported for the enzyme from soybean root nodules (0.5 mM for L-Glu and 60 µM for 3PHP [28]). K_m values at pH 8.2 were similar to PSAT from *E. coli* (1.2 mM for Glu and 4 µM for 3PHP [14]) and bovine liver (1.2 mM for Glu and 5 µM for 3PHP [21]). However, a markedly different K_m value for 3PHP has been observed for PSAT from sheep brain (0.25 mM [17]). However, the K_m values from the alkaliphiles do not indicate any specific deviation from general line among PLP -dependent enzymes and the differences can be explained by specific role of PSATs in the metabolism, like in the brain (Table 3). The Michaelis constants are indicative to substrate concentrations inside the cell of alkaliphiles.

The first-order rate constant, k_{cat}, was determined from the equation:

$$k_{cat} = {}_{obs}V_{max}/[E]_t \qquad (12)$$

in which ${}_{obs}V_{max}$ is observed velocity (M s^{-1}) at saturating substrate concentrations and $[E]_t$ is the stoichiometric concentration (M) of catalytic centres of PSAT. The k_{cat}/

Table 4: Amino acid analysis of PSAT-BALC, PSAT-BCIRA, PSAT-ECOLI, and PSAT from B. subtilis. Structural alignment was done with SwissProt. Abbreviations: D, aspartic acid; E, glutamic acid; H, histidine; K, lysine; N, asparagine; R, arginine; and Q, glutamine.

Enzyme	lenght (amino acids)	similarity (%)	DERK (charged) (%)	DE (negatively charged) (%)	RK (positively charged) (%)	HNQ (neutral hydrophilic) (%)
PSAT-BALC	361	100	19.1	10.3	8.9	16.6
PSAT-BCIRA	361	56	20.7	11.3	9.4	11.9
PSAT-ECOLI	362	42	22.2	12.2	10.0	10.3
PSAT-BSUB	359	59	23.1	12.5	10.6	11.7

K_m values for Glu and 3PHP at pH 8.2 were 27.5 x 10^3 $M^{-1}s^{-1}$ and 22.9 x 10^6 $M^{-1}s^{-1}$, and at pH 9.5 they were 70.2 x 10^3 $M^{-1}s^{-1}$ and 3.4 x 10^6 $M^{-1}s^{-1}$, in that order. These results only show the apparent general tendencies of kinetic parameters of the studied PSATs. To carry out a full kinetic analysis of all three enzymes will demand a separate, more detailed, but very laborious study.

Table 3 illustrates properties of PSAT-BALC and PSAT-BCIRA in comparison with the data on PSATs from other literature sources.

4 Discussion

Enzymes are favourable targets for studying the pH-adaptation of biomolecules since the active site can be sensitively monitored by its activity and characterized with established enzymological methods. PLP-dependent enzymes are especially favourable since PLP is itself a pH-indicator. Two evident main objects for the pH-adaptation of enzymes exist: the protein fold and the catalytic site, which may or may not be mutually interconnected. Apoenzyme-coenzyme interaction is a further subject of adaptation. A microbial cell should optimize the copy number of synthesized enzymes, their self-life, and catalytic activity to the prevailing pH conditions. The strategy how a microbe may choose the strategy to adopt the alkaline niche can be complex and a compromise.

The number of different microbial species is centred around "optimal" physical and chemical conditions which prevail in most places on the earth. When deviating from this optimum, the number of species drop down sharply. There are good reasons to ask: is the metabolic rate of a microbe living in extreme conditions (like in alkaline) slower than in "optimal conditions"? A microbe could afford having a slow metabolic rate in the absence of high microbial competition. Growth rate is a poor measure since it includes other parameters, including different numbers of enzyme molecules/cell. The turnover rates of enzymes can be straightforwardly compared. This question appears simple but to our knowledge has not been tried to be exactly answered. Different studies use different experimental conditions and enzymes of different purities, so that in practices the comparison from the literature can hardly even provide even an approximate answer. Since the present study was carried out with highly purified enzymes and activities measured in similar conditions, it was possible to compare the specific activities. The only striking difference between PSATs from alkaliphilic and neutrophilic organisms was the narrower and elevated pH optimum of the catalytic activity with the enzymes from the alkaliphiles. However, this may not deal with other enzymes and more related data are needed.

4.1 Catalytic pH optimum, optimal growth pH and apparent pH_i

The pH optima of the activity of PSATs from the facultative and obligate alkaliphiles were close to each other. We have observed that the pH of the growth medium of the alkalophilic *B. circulans* decreases rapidly in aerobic fermentation conditions from 10.5 to 8 by introduction of acids into the medium but after that the pH increases to about 9.5 [36]. Since the alkaliphilic PSATs had catalytic pH optima also at this pH region, it is conceivable that the pH optima of the intracellular enzymes are averaged around that operative pH_i. The catalytic pH optimum of *E. coli* PSAT also was close to the optimal growth pH of *E. coli*. The pH optima of intracellular enzymes have been frequently suggested to reflect pH_i [37] and this is rather common opinion among scientists. In spite of that, the pH optimum of cyclodextrin glucanotransferase from alkalophilic *B. circulans* was only 6.8. It could be explained by being a secreted enzyme and not aimed to function inside the cell [38].

4.2 Need for stabilization of protein fold and coenzyme binding?

The alkali-stability of the two PSATs of alkaliphilic *Bacillus* strains and *E. coli* were studied by keeping the enzymes at high and low pHs and measuring kinetics of the disappearance of the activity. All the three enzymes showed similar kinetics (indicating similar pH-dependent denaturation steps) and stabilities were practically the same (Figure 6). Denaturation occurred in the typical pH values for protein folds. This implies that there are no special structural arrangements for stabilization of the intracellular PSATs from alkaliphiles. The trend of usage of neutral amino acids (Table 4) may fall into statistical variation of the amino acids.

It is conceivable that a tighter binding of the coenzyme to apoenzyme would be necessary with the alkali-active enzymes. Notably sharp isosbestic points in the electronic spectra even up to pH 11.5 prove that the coenzyme was not liberated, or the locus of active site was not chemically altered (Figure 4). Thus, the activity drop in alkaline was due to the enzyme active site and not to detachment of PLP from apoenzyme or denaturation of the protein fold. However, it is questionable whether any extracellular PLP-containing enzyme could survive for a longer time active at above pH 11-12. PLP most probably stabilizes the protein fold like in other aminotransferases. Enzymes active in very alkaline conditions are possibly limited to hydrolytic non-cofactor reactions having more unique stabilized structures.

Extracellular high-alkaline serine M-protease from alkaliphilic *Bacillus* has been reported to have increased levels of Asn, Gln, His and Arg and less of Asp, Glu and Lys in comparison with related less alkaline enzymes [39]. Some of the Arg residues form additional hydrogen bonds or ion pairs to combine both N- and C-terminal regions of M-protease. Furthermore, in the crystal, M-protease has a salt bridge between Arg19, Arg269, and Glu265, which is located on the opposite side from the catalytic site [39, 40]. These two Arg residues are found only in high-alkaline proteases, and such a salt bridge is the one that is often present characteristically in the high-alkaline enzymes [41]. Alkaline active xylanases tend to have a high percentage of acidic amino acids [42]. Similar conclusions were drawn based on nitrite reductases from bacteria growing in alkaline and high salinity [43]. In very high salinity, it is reasonable that the salt bridges on the surface in the enzyme enable the solubility of the enzyme. Otherwise the protein could be "salted-out" and precipitate. In the present study with intracellular PSATs the adaptation of the protein fold to alkaline was minor. The three PSATs here all had the same p*I* of 4.6 meaning that surface charge was similar even though the distribution pattern of the charges could be different as found with xylanases [42]. The adaptation mechanism is most probably different in moderately alkaline and high-alkaline conditions.

4.3 pKa of aldimine nitrogen

Hayashi and co-workers [34, 44] proposed that the major determinant of the low aldimine pK_a of AspAT origins from the imine-pyridine torsion angle of the Schiff base. In HPAT, the molecular strain of the Schiff base was shown to be the principal factor for the low pK_a (6.6). Such a molecular strain is common to the subgroup I aminotransferases (e.g. AspAT and HPAT). The molecular distortion breaks the intramolecular hydrogen bond between O3' of PLP and the distal N of Lys258, and the conjugation between the π-orbitals of the imine and pyridine ring. As a result, the protonated form is strongly destabilized and the unprotonated form stabilized. Hayashi et al. [34] considered, that in AspAT, and other PLP enzymes, as well, Lys C(α)-PLP C4' distance and the position of Cα relative to PLP (torsion angle of C3-C4-C4'-Cα) determines the strain of the PLP aldimine.

4.4 Strain of the internal aldimine of the unliganded enzyme

Based on existing literature data, the Cα-C4' distances in PSAT-BCIRA dimer (PDB accession number 1BT4) are 6.18 Å in both chain, A and B, and in PSAT-ECOLI dimer (1BJN) 6.85 Å in A chain and 7.04 Å in B chain. The torsion angle of the PLP-Lys aldimine, C3-C4-C4'-C(α), for PSAT-BCIRA A and B chain are 47.47° and 47.42°, respectively. Correspondingly, in PSAT-ECOLI angles are 45.85° and 43.92°. In AspAT-ECOLI (1ARS) C(α)-C4' distance is 7.08 Å and torsion angle 95.91° [34]. Torsion parameters of PSAT-BCIRA, PSAT-ECOLI and AspAT-ECOLI are shown in Table 5. A considerably lower torsion angle in PSAT-ECOLI explains the pK_a of internal aldimine in comparison to AspAT. Moreover, higher pK_a in PSAT-BCIRA than in PSAT-ECOLI is well explained by the impact of shorter C(α)-C4' distance on PSAT-BCIRA (which is reflected in the pK_a of internal aldimine). The source of adaptation of PSATs to pH can be explained on a molecular level by the differences in the torsion angles of the coenzyme (shown by the pK_a). How these torsion angles are realized in the molecular

Table 5: Factors that determine the torsion angle of the PLP-Lys aldimine. Column PDB refers to Protein Data Bank accession code: 1BT4, PSAT-BCIRA dimer; 1BJN, PSAT-ECOLI dimer; and 1ARS, AspAT dimer of *E.coli*.

PDB code	C(α)-C4' (Å)	C3-C4-C4'-C(α) (deg)
1BT4	6.18	47.42
1BJN	6.85-7.04	43.92-45.85
1ARS	7.08	95.91

level by the enzyme active sites could be answered by the 3-D studies.

All the PLP -dependent enzymes have conserved secondary structures and the phosphate group of PLP locates at the end of a terminal alpha helix with a special motif of "phosphate binding cup" ([45], see also the references therein). Very surprisingly, all PLP-dependent enzymes, even glycogen phosphorylase with different function of PLP, have extensive common structural segments of the polypeptide chain responsible for the appropriate disposition of the key residues inside the enzyme. In spite of these common elements, it is considered that all the proteins do not have mutual heritage but have arisen on five separate occasions [46]. These findings connected to our early notification for structural and chemical resemblance between PLP and pyrimidine bases [47] is of interests in understanding the evolutionary link between PLP-dependent proteins and nucleic acids. Nature has sometimes elected only certain highly conserved motifs, like secondary structures of PLP-dependent enzymes and phosphate binding. For the rest parts of residues, a wide freedom to choose functional alternatives exists as shown by the lack of almost all sequence homology.

4.5 Brief comments onto 3-D structures of PSATs from alkaliphiles

There are a number of 3-D structures of PSATs resolved (see e.g. [48] and the references therein; Table 5). The adaptation of PSATs to alkaline pH was studied by comparing 3-D structure of PSAT of *B. circulans* var. *alkalophilus* [7] with previously solved structure of PSAT from *E.coli* [5]. The general structural features were almost the same in both PSATs [7]. Possible explanations, like a tighter structure of the active site of the alkali-active enzyme were ruled out. The shift of the pH optimum to alkaline direction was explained by the additional hydrogen bonds to O3′ of PLP with the enzymes from alkaliphilic microbes [7]. The X-ray method has many advantages but also drawbacks like a very tedious and unpredictable way to get crystals for solving the predetermined task, for example difficulty to get diffracting crystals at different pHs or to crystallize intermediates.

The paper by Sekula et al. [48] describes 3-D structures of three intermediate structures of PSAT from plant source. The finding that crystallization of PSAT with substrate in the absence of sulphate (competing with the phosphate binding site of PSer) can "freeze" the geminal diamine intermediate is unique. The step is extremely fast in a non-enzymic model, as well as in enzymic reactions and therefore the intermediate is usually possible to detect only kinetically. However, we were able to observe directly a cyclic geminal diamine in the reaction of the O-amino serine and PLP in alkaline solution by NMR [49] demonstrating that the disruption of the geminal diamine is acid catalysed while in lower pHs the reaction could be shown only kinetically. Battula et al. [8] found external aldimine intermediate of PSer in PSAT co-crystallization with the substrate PSer. As far as we know, nobody else has found such an intermediate since the reaction takes place also in crystals. All previous studies have used non-productive substrate analogues in such studies. There were not found to be typical conformational changes for bound substrates at the active site. Evidently such studies could be done more conveniently and simply with spectrophotometry or done parallelly. If the crystal itself was the origin of the exceptional "frozen" structures, then the absorption spectra of crystal suspensions (or single crystals) can be used. Tris- buffer should be avoided in all studies with PLP enzymes since Tris reacts with the coenzyme.

4.6 Role of protons in the PSAT activity profiles

The pK_a value of the amino group of PSer is 9.0. At around the pH optimum of activity of PSATs from the alkaliphiles the statistical number of protons entering the active site with substrate is strongly dependent on the pH. At the pH optimum of the activity the PSAT active site is half-protonated, i.e. in equilibrium between two ionic species (Figure 4 and 5). The equilibrium is fast but not enough to be detected on NMR time scale (averaged) while it can be detected with spectrophotometry. Thus, the catalysis optimum occurs in an unstable pH region of PSAT active site. Catalysis of all PLP enzymes is dependent on a certain correct number of protons at the active site. In neutral pH, each amino acid brings, on the average, one

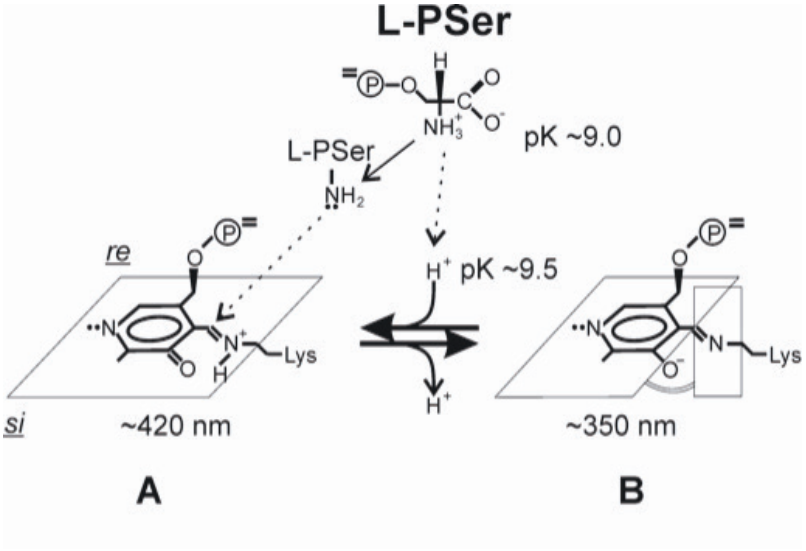

Figure 7: A schematic presentation of the initial step of the reaction of L-PSer with PSAT active site. The structures of PLP ketoenamine (A) and enolimine (B) are drawn schematically not considering possible mesomeric structures or connections to apoenzyme. In (A) the planar structure includes the azomethine nitrogen with Lysine residue. When the azomethine nitrogen loses proton (pK_a 9.5), this planarity is lost (B) and the azomethine bond makes another plane with an angle to plane (A). During the reaction, the amino group of the substrate (PSer or Glu) should attach to carbon C4´ shown by arrow in (A) since that carbon is distinctly more electropositive than the same carbon in (B). The pK_a of the parent PSAT chromophore (9.5) is the fact shown by the titration data. It has certainly structural reasons (hydrogen bonds to apoenzyme etc) shown by the X-ray data. Why the maximum catalytic activity appears very exactly at the same pH-value as the pK_a of the chromophore remains unclear. An additional problem is how to explain that the specific activities of alkali-active enzymes are practically the same as with PSAT from *E. coli*. The nucleophilic attack of a substrate should take place by the deprotonated amino group to C4´ (to form the first covalent bond, the geminal diamine intermediate). High pH values favour existence of deprotonated substrate amino groups but disfavour the population of enzymes capable to the nucleophilic attack. This scheme speculates that substrates transfer protons into the active site and locate to the azomethine nitrogen. After the geminal diamine, the next reaction steps are formation of external aldimine, abstraction of alpha-hydrogen from the substrate and production of pyridoxamine form of coenzyme and ketoacid.

proton into the active site. Anticipatedly, it is delocalized from the amino group near to the imino nitrogen of the active site (assumed in ref. 33; see also ref. 33 Figures 14-39). At the pH optimum of the alkaline-active PSATs, if non-aminoprotonated PSer will enter the active site it can abstract a proton from the active site and change the active site to a non-protonated form. If a protonated PSer enters the active site it can donate a proton to the non-protonated active site. At the pH optimum, the velocity of interchange of the ionic forms are fast (but detectable with the time scale of electronic spectra). If the substrate brings any proton to the active site it is beneficial to the reaction. Figure 7 schematically shows that idea. If there were a water mediated channel, protons could escape from the active site rather than transferred against a pH gradient and therefore active site should be also isolated from the bulk water during the catalysis.

The narrow pH optimum of the alkaliphilic enzymes could be due to the fact that enzyme active centre requires catalytic proton(s). If they are not brought in by the substrate, they must be stored outside the critical functional groups and then moved back, or protons must be transferred otherwise from the bulk solvent which is difficult to imagine. One way to organize the required protonation stage is by adjustment of the chemical milieu of the active site. If the amino proton from PSer (or Glu) is required for the catalysis, the solvent conditions must be hydrophilic during the entrance of the substrate to the active site (to keep pK of the amino group close to the one in water) and finally more hydrophobic to release the proton. In non-polar conditions of (d_4-) methanol alpha nitrogen and alpha carboxyl can share the proton of the Schiff´s base [50]. Except in the case of solvent effects, term pH should be interpreted with care in the context of biomolecules since the proton ion activity on or inside a protein may differ drastically from that in aqueous solution. The apparent pH of the active site of PLP enzymes may rather resemble methanol than water. In such conditions pK_a values of amino and carboxylic group of Schiff´s bases can be reversed [9, 51]. Protonation of phosphate group of PLP bound to AspAT apoenzyme cannot be detected because of very low pK_a. Instead,

conformational changes of the phosphoric acid ester bond is very useful is studying the active site with ^{31}P NMR [52]. ^{31}P NMR is an excellent tool to study the conformational changes of PLP in the active site together with the electronic absorption spectra and circular dichroism. In the case of PSer, substrate binding and reaction could be followed ^{31}P NMR. The spectrophotometrically (or with ^{31}P NMR) titratable pK_a of the PLP chromophore is a complex (non-linear function of the reaction pathway) of the pH measured from the bulk solvent. The high dependence of PSAT activity on the buffer anions (Figure 3) most probably reflects contribution of certain buffers to proton transfers with the active site. This is a long-known phenomenon with the PLP-dependent enzymes and shows the crucial role of protons in the catalysis. The very high side activity of alkali-active PSATs to aspartate may be understandable (see Introduction) since aspartate has a higher pK_a (about 9.9) of the amino nitrogen than Pser or Glu and therefore could be a better carrier of protons to the active site. This supports the suggestion of a need of transfer of one proton to the active site.

Aminotransferases use "movable" protons for promoting the catalytic act. In the case of AspAT, it could be brought by the substrate amino group. Logically, such a proton is donated to the imino nitrogen since then the electropositivity of C4` of PLP increases and concomitantly then the nucleophilicity of the amino group of the substrate increases [33]. The step leading to the product must be concerted and timed with other movements of the functional groups/conformational changes (including "open and close conformations") at the active site. The act is principally different from catalysis in solutions. This view also necessitates that the enzyme active site is shielded from free access of protons (and water) and that the substrate can induce productive (non-random) catalytic events. Accordingly, the whole catalytic act shall proceed in a time synchrony: if the proton is brought by the substrate it will induce the next step of the act. The optimally productive catalytic act is a sequence of steps enabling the next step to occur, i.e. the overall catalytic act is like a stepwise set of events under a time control whatever fast the reaction is. With the PLP-dependent enzymes these steps are well established protons transfers described in textbooks (see e.g. [10]).

The two enzymes from alkaliphilic microbes showed quite similar pH optima for the forward reaction with substrate PSer. This was possibly due to adaptation of the enzymes to similar cellular pH_i values which furthermore coincided with the chromophore pK_a values. The PSATs from the alkaliphiles behaved equally in many respects with exception of difference of protonation of the ES complexes and differences in molar absorptivities of the PLP chromophore. The suggested view of transfer of protons with the substrate discussed includes when the pH is increased clearly above the pK_a of the amino group of substrates, active centre cannot compensate the lack of protons conveyed by the substrate. High concentration of buffers can have an effect but this may be an artificial effect because this is not due to situation *in vivo*.

5 Conclusions

Enzymatic properties of homologous, practically pure intracellular PSATs, from neutralophilic and alkaliphilic microbes were studied in equal conditions by enzyme kinetic methods and by spectrophotometric titration. When the enzyme activities were measured at similar conditions at optimal pHs, the specific activities were the same. The enzymes from alkaliphilic microbes have to "pay" for the alkaline conditions only by a narrower pH optimum of activity. The PSATs from alkaliphiles have unique properties which deserve additional and more careful kinetic studies and studies with spectrophotometry, CD, ^{31}P NMR and other NMR methods.

Acknowledgements: This study was performed by the funding from The Joint Biotechnology Laboratory of the University of Turku, Finland and by a grant from Academy of Finland #321762.

Conflict of interest statement: The authors do not know any conflict of interest.

References

[1] Battchikova N, Himanen JP, Ahjolahti M, Korpela T. Phosphoserine aminotransferase from Bacillus circulans subsp. alkalophilus: purification, gene cloning and sequencing. Biochim Biophys Acta. 1996a Jul;1295(2):187–94.

[2] Battchikova N, Koivulehto M, Denesyuk A, Ptitsyn L, Boretsky Y, Hellman J, et al. Aspartate aminotransferase from an alkalophilic Bacillus contains an additional 20-amino acid extension at its functionally important N-terminus. J Biochem. 1996b Aug;120(2):425–32. Available from: https://www.jstage.jst.go.jp/article/biochemistry1922/120/2/120_2_425/_pdf/-char/en

[3] Kravchuk Z, Tsybovsky Y, Koivulehto M, Vlasov A, Chumanevich A, Battchikova N, et al. Truncated aspartate aminotransferase from alkalophilic Bacillus circulans with deletion of N-terminal 32 amino acids is a non-functional monomer in a partially structured state. Protein Eng. 2001 Apr;14(4):279–85.

[4] Moser M, Müller R, Battchikova N, Koivulehto M, Korpela T, Jansonius JN. Crystallization and preliminary X-ray analysis of phosphoserine aminotransferase from Bacillus circulans subsp. alkalophilus. Protein Sci. 1996 Jul;5(7):1426–8.
[5] Hester G, Stark W, Moser M, Kallen J, Marković-Housley Z, Jansonius JN. Crystal structure of phosphoserine aminotransferase from Escherichia coli at 2.3 A resolution: comparison of the unligated enzyme and a complex with alpha-methyl-l-glutamate. J Mol Biol. 1999 Feb;286(3):829–50.
[6] Dubnovitsky AP, Kapetaniou EG, Papageorgiou AC. Expression, purification, crystallization and preliminary crystallographic analysis of phosphoserine aminotransferase from Bacillus alcalophilus. Acta Crystallogr D Biol Crystallogr. 2003 Dec;59(Pt 12):2319–21.
[7] Dubnovitsky AP, Kapetaniou EG, Papageorgiou AC. Enzyme adaptation to alkaline pH: atomic resolution (1.08 A) structure of phosphoserine aminotransferase from Bacillus alcalophilus. Protein Sci. 2005 Jan;14(1):97–110.
[8] Battula P, Dubnovitsky AP, Papageorgiou AC. Structural basis of L-phosphoserine binding to Bacillus alcalophilus phosphoserine aminotransferase. Acta Crystallogr D Biol Crystallogr. 2013 May;69(Pt 5):804–11.
[9] Christen P, Metzler DE. Transaminases. Biochemistry, A Series of Monographs. 2nd ed. New York: John Wiley & Sons; 1985.
[10] Metzler DE. Pyridoxal Phosphate. In: Metzler DE, editor. Biochemistry. The Chemical Reactions of Living Cells. Volume 1. 2nd ed. Harcourt Academic Press; 2001. pp. 737–53.
[11] Mattsson P, Battchikova N, Sippola K, Korpela T. The role of histidine residues in the catalytic act of cyclomaltodextrin glucanotransferase from Bacillus circulans var. alkalophilus. Biochim Biophys Acta. 1995 Feb;1247(1):97–103.
[12] Tabor S, Richardson CC, Bacteriophage A. A bacteriophage T7 RNA polymerase/promoter system for controlled exclusive expression of specific genes. Proc Natl Acad Sci USA. 1985 Feb;82(4):1074–8.
[13] Sambrook J, Fritch EF, Maniatis T. Molecular cloning: a laboratory manual. 2nd ed. Cold Spring Harbor, New York: Cold Spring Harbor Laboratory Press; 1989.
[14] Lewendon A. Doctoral Thesis, University of Glasgow; 1984.
[15] Bradford MM. A rapid and sensitive method for the quantitation of microgram quantities of protein utilizing the principle of protein-dye binding. Anal Biochem. 1976 May;72(1-2):248–54.
[16] Laemmli UK. Cleavage of structural proteins during the assembly of the head of bacteriophage T4. Nature. 1970 Aug;227(5259):680–5.
[17] Hirsch H, Greenberg DM. Studies on phosphoserine aminotransferase of sheep brain. J Biol Chem. 1967 May;242(9):2283–7.
[18] Guex N, Peitsch MC. SWISS-MODEL and the Swiss-PdbViewer: an environment for comparative protein modeling. Electrophoresis. 1997 Dec;18(15):2714–23.
[19] Schwede T, Kopp J, Guex N, Peitsch MC. SWISS-MODEL: an automated protein homology-modeling server. Nucleic Acids Res. 2003 Jul;31(13):3381–5.
[20] Peitsch MC. Protein modeling by E-mail, Bio/Technol. 1995;13:658-60.
[21] Lund K, Merrill DK, Guynn RW. Purification and properties of phosphoserine aminotransferase from bovine liver. Arch Biochem Biophys. 1987 Apr;254(1):319–28.
[22] Dixon M, Webb EC. Enzymes. 2nd ed. New York: Academic Press; 1964. pp. 116–66.
[23] Segel IH. Enzyme kinetics. Behaviour and analysis of rapid equilibrium and steady-state enzyme systems, John Wiley & Son; 1975.
[24] Alberty RA, Massey V. On the interpretation of the pH variation of the maximum initial velocity of an enzyme-catalyzed reaction. Biochim Biophys Acta. 1954 Mar;13(3):347–53.
[25] Kallen J, Kania M, Markovic-Housley Z, Vincent MG, Jansonius JN. Crystallographic and solution studies on phosphoserine aminotransferase (PSAT) from E. coli. In: Korpela T, Christen P, editors. Biochemistry of Vitamin B6. Basel: Birkhäuser Verlag; 1989. pp. 157–60.
[26] Basurko MJ, Marche M, Darriet M, Cassaigne A. Phosphoserine aminotransferase, the second step-catalyzing enzyme for serine biosynthesis. IUBMB Life. 1999 Nov;48(5):525–9.
[27] Stolz M, Dornemann D. Kinetic characteristics, substrate specificity and catalytic properties of phosphoserine aminotransferase from the Green Alga Scenedesmus obliquus, Mutant C-2A. Z. Naturforsch. 1995;50c(9-10):630–7.
[28] Reynolds PH, Hine A, Rodber K. Serine metabolism in legume nodules: purification and properties of phosphoserine aminotransferase. Physiol Plant. 1988;74(1):194–9.
[29] Sung MH, Tanizawa K, Tanaka H, Kuramitsu S, Kagamiyama H, Soda K. Purification and characterization of thermostable aspartate aminotransferase from a thermophilic Bacillus species. J Bacteriol. 1990 Mar;172(3):1345–51.
[30] John RA. Pyridoxal phosphate-dependent enzymes. Biochim Biophys Acta. 1995 Apr;1248(2):81–96.
[31] Jansonius JN, Vincent MG. Structural basis for catalysis by aspartate aminotransferase. In: Jurnak FA, McPherson A, editors. Active Sites of Enzymes. Volume 3. New York: John Wiley & Sons; 1987. pp. 187–285.
[32] Mizuguchi H, Hayashi H, Miyahara I, Hirotsu K, Kagamiyama H. Characterization of histidinol phosphate aminotransferase from Escherichia coli. Biochim Biophys Acta. 2003 Apr;1647(1-2):321–4.
[33] Makela MJ, Korpela TK. Chemical models of enzymic transimination. Chem Soc Rev. 1983;12(3):309–29.
[34] Hayashi H, Mizuguchi H, Miyahara I, Islam MM, Ikushiro H, Nakajima Y, et al. Strain and catalysis in aspartate aminotransferase. Biochim Biophys Acta. 2003 Apr;1647(1-2):103–9.
[35] Velick SF, Vavra J. A kinetic and equilibrium analysis of the glutamic oxaloacetate transaminase mechanism. J Biol Chem. 1962 Jul;237:2109–22.
[36] Paavilainen S, Oinonen S, Korpela T. Catabolic pathways of glucose in Bacillus circulans var. alkalophilus. Extremophiles. 1999 Nov;3(4):269–76.
[37] Abe F, Horikoshi K. The biotechnological potential of piezophiles. Trends Biotechnol. 2001 Mar;19(3):102–8.
[38] Makela M, Mattsson P, Schinina M, Korpela T. Purification and properties of cyclomaltodextrin glucanotransferase from an alkalophilic Bacillus. Biotechnol Appl Biochem. 1988;10:414–27.
[39] Shirai T, Suzuki A, Yamane T, Ashida T, Kobayashi T, Hitomi J, et al. High-resolution crystal structure of M-protease: phylogeny aided analysis of the high-alkaline adaptation mechanism. Protein Eng. 1997 Jun;10(6):627–34.

[40] Yamane T, Kani T, Hatanaka T, Suzuki A, Ashida T, Kobatashi T, et al. Structure of a new alkaline serine protease (M-protease) from Bacillus sp. KSM-K16. Acta Crystallogr D Biol Crystallogr. 1995 Mar;51(Pt 2):199–206.
[41] Ito S, Kobayashi T, Ara K, Ozaki K, Kawai S, Hatada Y. Alkaline detergent enzymes from alkaliphiles: enzymatic properties, genetics, and structures. Extremophiles. 1998 Aug;2(3):185–90.
[42] Mamo G, Thunnissen M, Hatti-Kaul R, Mattiasson B. An alkaline active xylanase: insights into mechanisms of high pH catalytic adaptation. Biochimie. 2009 Sep;91(9):1187–96.
[43] Popinako A, Antonov M, Tikhonov A, Tikhonova T, Popov V. Structural adaptations of octaheme nitrite reductases from haloalkaliphilic Thioalkalivibrio bacteria to alkaline pH and high salinity. PLoS One. 2017 May;12(5):e0177392.
[44] Hayashi H, Mizuguchi H, Kagamiyama H. The imine-pyridine torsion of the pyridoxal 5′-phosphate Schiff base of aspartate aminotransferase lowers its pKa in the unliganded enzyme and is crucial for the successive increase in the pKa during catalysis. Biochemistry. 1998 Oct;37(43):15076–85.
[45] Denesyuk AI, Denessiouk KA, Korpela T, Johnson MS. Functional attributes of the phosphate group binding cup of pyridoxal phosphate-dependent enzymes. J Mol Biol. 2002 Feb;316(1):155–72.
[46] Denessiouk KA, Denesyuk AI, Lehtonen JV, Korpela T, Johnson MS. Common structural elements in the architecture of the cofactor-binding domains in unrelated families of pyridoxal phosphate-dependent enzymes. Proteins. 1999 May;35(2):250–61.
[47] Kurkijärvi K, Raunio R, Korpela T. Spectrophotometric titrations of micellar Schiff's bases prepared from pyridoxal 5′-phosphate. Int J Biol Macromol. 1981;3(6):389–94.
[48] Sekula B, Ruszkowski M, Dauter Z. Structural analysis of phosphoserine aminotransferase (isoform1) from Arabidopsis thaliana-the enzyme involved in the phosphorylated pathway of serine biosynthesis. Front Plant Sci. 2018 Jul;9:876.
[49] Korpela T, Mäkelä M, Lönnberg H. Spectroscopic and kinetic evidence for a cyclic geminal diamine intermediate in the reaction of O-aminoserine with pyridoxal 5′-phosphate in alkali. Arch Biochem Biophys. 1981 Dec;212(2):581–8.
[50] Mäkelä M, Hormi O, Jula E, Korpela T. Acid-base titrations of schiff bases in deuteriomethanol as studied by1H NMR. J Solution Chem. 1989;18:691.
[51] Lehtokari M, Puisto J, Raunio R, Korpela T. Spectrophotometric titrations of pyridoxal Schiff's bases in methanol using glass electrode for control of acidity. Arch Biochem Biophys. 1980 Jul;202(2):533–9.
[52] Korpela T, Mattinen J, Himanen JP, Mekhanic ML, Torchinsky YM. Phosphorus-31 nuclear magnetic resonance of aspartate aminotransferase from chicken heart cytosol. Biochim Biophys Acta. 1987 Sep;915(2):299–304.
[53] Demirjian DC, Morís-Varas F, Cassidy CS. Enzymes from extremophiles. Curr Opin Chem Biol. 2001 Apr;5(2):144–51.
[54] Eichler J. Biotechnological uses of archaeal extremozymes. Biotechnol Adv. 2001 Jul;19(4):261–78.
[55] Niehaus F, Bertoldo C, Kähler M, Antranikian G. Extremophiles as a source of novel enzymes for industrial application. Appl Microbiol Biotechnol. 1999 Jun;51(6):711–29.
[56] Rothschild LJ, Mancinelli RL. Life in extreme environments. Nature. 2001 Feb;409(6823):1092–101.
[57] Booth IR. The regulation of intracellular pH in bacteria, in D.J. Chawdick, G. Cardew (Eds.), Bacterial Responses to pH, Novartis Found. Symp., Wiley-Blackwell, Chichester, England. 1999;221:19-28.
[58] Krulwich TA, Guffanti M, Ito M. pH Tolerance in Bacillus: alkaliphiles versus non-alkaliphiles, in D.J. Chawdick, G. Cardew (Eds.), Bacterial Responses to pH, Novartis Found. Symp., Wiley-Blackwell, Chichester, England, 1999, Vol. 221, pp, 167-179.
[59] Horikoshi K. Alkaliphiles: some applications of their products for biotechnology. Microbiol Mol Biol Rev. 1999 Dec;63(4):735–50.